



JOINT INSTITUTE FOR NUCLEAR RESEARCH

Dzelepov Laboratory of Nuclear Problems

**FINAL REPORT ON THE
SUMMER STUDENT PROGRAM**

**Evaluation of the influence of the light field in containers
for PMT mass testing on the sensitivity of the JUNO
experiment**

Supervisors:
Tatiana Antoshkina
Maxim Gonchar

Student:
Dmitry Dolzhikov

Participation period:
June 25 – August 20

Dubna, 2017

Contents

Abstract	2
Introduction	3
1 JUNO experiment	4
1.1 JUNO Detector	4
1.2 PMT mass-testing methods	6
1.2.1 Container approach	6
1.2.2 Scanning station	7
2 Studying of the light field distribution in the container	9
2.1 Preliminary measurements	10
2.1.1 Angular distribution of teflon plate	10
2.1.2 The study of the angular transmittance of angular selective transmission device (ASTD)	10
2.2 Small PMT approach	12
2.3 Camera approach	14
2.3.1 The construction of a characteristic curve between the values of a small PMT and the camera	14
2.3.2 Production and processing of photos	16
2.4 Estimation of the contribution to the LFD by diffuse light from tyvek	19
Conclusion	21
Bibliography	22

Abstract

This paper is devoted to the investigation of the light field distribution in cylinders (in the container system) for the 20-inch PMTs for the JUNO detector.

We present results of the measurement of the angular distribution of the diffuser with a light source (teflon plate and self-calibrating LED). The angular transmittance of the angular selective transmission devices (ASTD) is investigated.

Two methods of the measurement of the light field are considered:

1. Using a small photomultiplier with an ASTD,
2. Using the camera.

An estimate of the impact of the light scattered by tyvek to the global light field distribution in the cylinder is given.

Introduction

In recent years more and more experiments aimed at studying neutrinos have appeared. Most of these experiments use neutrino detectors. Huge collaborations are engaged in the design, construction, testing and maintenance of the neutrino detectors. In this paper the JUNO project is considered — in particular the methods for testing the large number of photomultiplier tubes (PMT) that will be used in this project and the application limits of these methods in practice.

Chapter 1

JUNO experiment

Jiangmen Underground Neutrino Observatory (JUNO) is a reactor antineutrino experiment under construction in Jiangmen City, Guangdong Province, China. The JUNO detector will mostly receive $\bar{\nu}_e$ from two reactor complexes at Taishan and Yangjiang. The average baseline of JUNO is 52.5 km with a RMS¹ of 0.25 km. The experiment aims to achieve an energy resolution of better than 1.9% at 2.5 MeV (or 3% at 1 MeV), which is essential for the neutrino mass hierarchy (MH) determination.

Nuclear power reactors produce electricity by the sustained nuclear chain reaction and are essentially pure electron antineutrino $\bar{\nu}_e$ sources. For each 1 gigawatt (GW) of the reactor thermal power about 2×10^{20} $\bar{\nu}_e$ are emitted isotropically every second making nuclear reactors one of the most powerful man-made neutrino sources.

JUNO is designed to resolve the neutrino MH using precise spectral measurements of reactor antineutrino oscillations.

1.1 JUNO Detector

The JUNO detector consists of a central detector, a water Cherenkov detector and a muon tracker. The central detector is a liquid scintillator (LS) detector of 20 kton fiducial mass with a designed energy resolution of $3\%/\sqrt{E(\text{MeV})}$. The central detector is submerged in a water pool to be shielded from natural radioactivity from the surrounding rock and air. The water pool is also equipped with PMTs to detect the Cherenkov light from cosmic muons, acting as a veto detector. On the top of the water pool there is another muon detector to accurately measure the muon tracks. A schematic view of the JUNO detector is shown in Fig. 1.1.

To achieve the required energy resolution it is necessary to fulfill the following requirements:

1. The central detector PMT photocathode coverage $\geq 75\%$,

¹root mean square

2. The PMT photocathode quantum efficiency $\geq 25\%$,
3. The attenuation length of the liquid scintillator is 20 m at 430 nm, which corresponds to an absorption length of 60 m with a Rayleigh scattering length of 30 m.

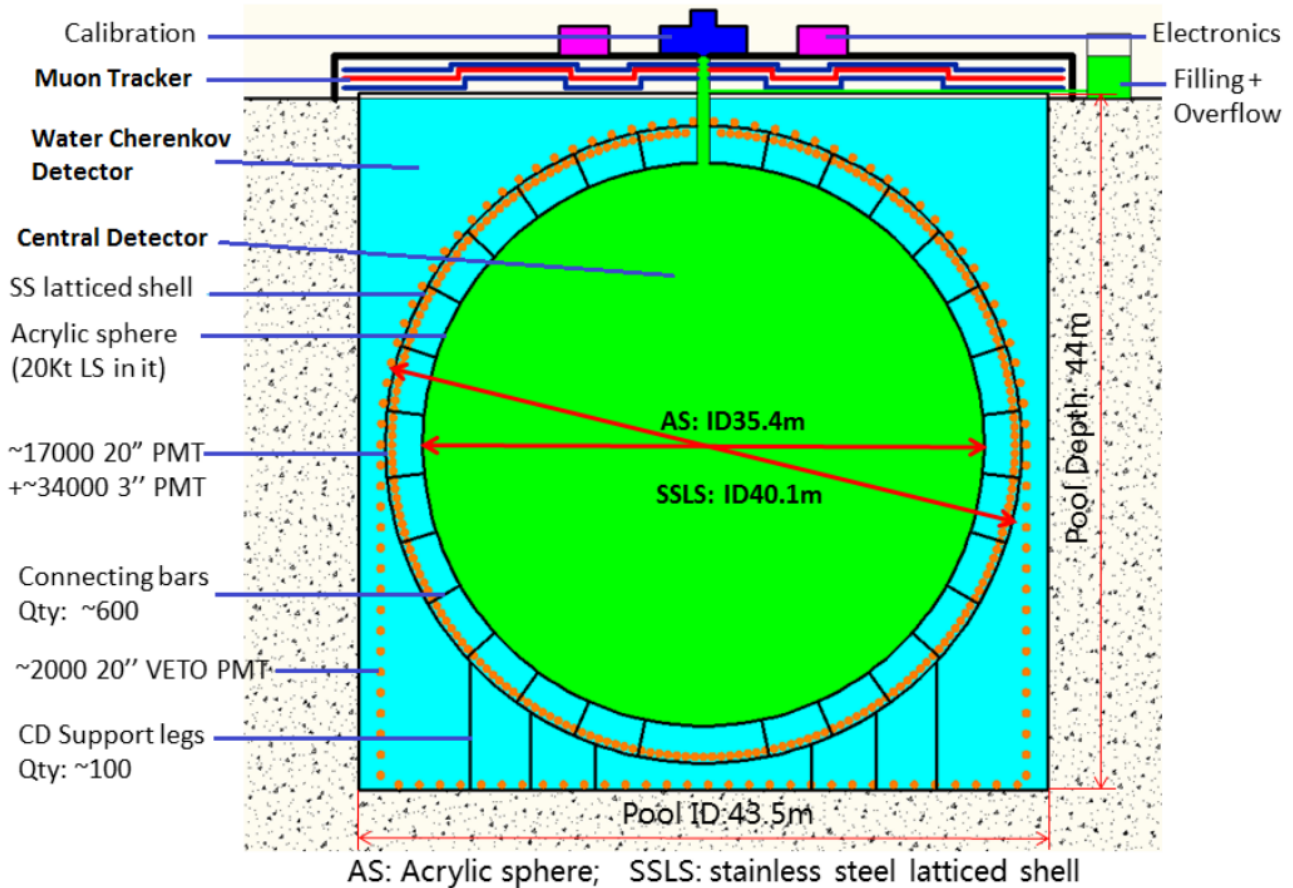


Figure 1.1: A schematic view of the JUNO detector.

The density of the LS is 0.859 g/ml. 20 kt LS is contained in a spherical container of radius of 17.7m. The light emitted by the LS is collected by about 17000 20-inch PMTs. PMTs are installed on a spherical structure of a radius of 19.5 m, and submerged in a buffer liquid to protect the LS from the radioactivity of the PMT glass.

The mechanics of the central detector is very challenging. The acrylic vessel is used to contain the LS of the central detector. The buffer liquid is water which is connected with the outer water Cherenkov detector but is optically separated. The PMTs are installed on the inner surface of the truss structure, which also supports the acrylic sphere.

The central detector is submerged in a cylindrical water pool. At least 2 m water from any direction protects the central detector from the surrounding rock radioactivity. About 1600 20-inch PMTs are installed in the water pool. The muon detection efficiency is expected to be 99.8%.

The earth magnetic field intensity is about 0.5 gauss at the experimental site. It could have significant negative impact on the photoelectron collection efficiency of the large size PMTs. Both compensation coils surrounding the water pool and high- μ metal shielding for individual PMTs will be installed.

On the top of the water pool the muon tracker will be installed to accurately measure the muon direction. Plastic scintillator strips decommissioned from the target tracker of the OPERA experiment will be reused as the JUNO top tracker. The OPERA target tracker is composed of 62 walls with a sensitive area of $6.7 \times 6.7 \text{ m}^2$ each. Each wall consists of four vertical (x) and four horizontal (y) modules. A target tracker module is composed of 64 scintillating strips, 6.7 m long and 26.4 mm wide. Each strip is read out on both sides by a Hamamatsu 64-channel multi-anode PMT. The total surface which could be covered by the 62 x-y walls is 2783 m^2 . Radioactivity from the surrounding rock of the experimental hall will induce extremely high noise rate in the plastic scintillator strips. Multi-layer design, at least 3 x-y layers, is needed to suppress the radioactivity background. Distance between two adjacent super-layers will be between 1 m and 1.5 m. The muon tracker will cover more than 25% of the area of the top surface of the water pool.

A chimney for calibration operation will connect the central detector to outside from the top. Special radioactivity shielding and muon detector will be designed for the chimney [1].

1.2 PMT mass-testing methods

1.2.1 Container approach

All of the 17000 large-photocathode 20-inch PMTs will be tested in 4 containers which are designed and produced by the team from the University of Hamburg and the University of Tübingen. Each container is a 20' refrigerated container that can control the temperature within a range between -20°C and 45°C with a precision of less than 1°C . In addition, the containers are lined with a multi-layer magnetic shielding based on silicon iron that guarantees a magnetic field of less than 10% of the EMF in each of the 36 measurement positions.

To provide identical and reproducible measurement conditions each container is equipped with 36 precision-made drawer boxes housed in a shelf, as can be seen in Fig. 1.2. The complete shelf system (including the boxes) is made from aluminum, and nearly all surfaces inside the container and the drawer boxes are black. The PMTs are placed on removable trays equipped with a precise holder made from anti-static foam. The trays are then fixed to the drawer by a clamping lever, allowing for the precise positioning of the PMTs inside each drawer.

On the other side of the drawer boxes the light sources are mounted 50 cm

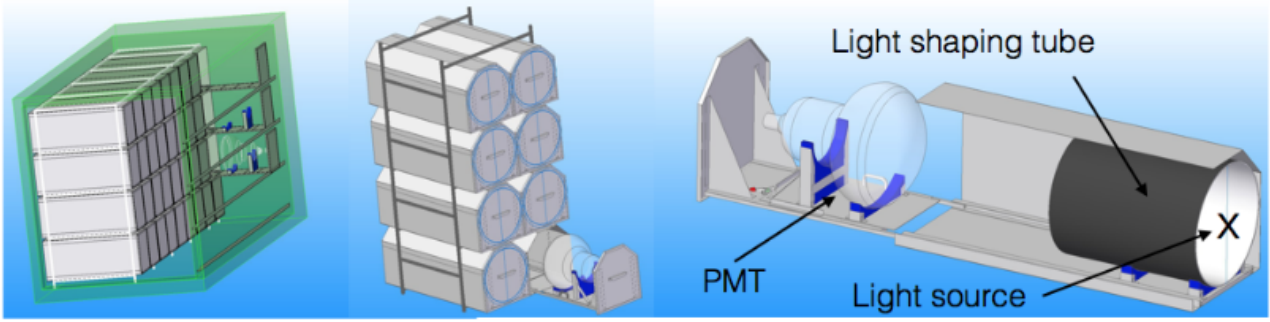


Figure 1.2: The Container: general view (left), drawers (middle), PMT layout in a drawer (right).

away from the top of the PMT. The light sources are stabilized LEDs produced by the HVSYS company, and are also used in the scanning stations. They are deployed behind optics (including a diffuser) designed to generate a suitable light field to illuminate the entire surface of the 20" PMTs with an intensity between 0.1 and 1.5 photons per LED pulse. A large light shaping tube, coated black on one side and equipped with highly reflecting Tyvek on the other side, ensures that the sides of the PMTs are also illuminated (see Fig.1.2 right). In addition, two of the four containers will be equipped with a picosecond Laser (wavelength of about 420 nm). The light of the lasers will be distributed by optical fibers producing a light field of similar intensity but within a narrower cone.

Not all of the PMT characteristics can be tested inside the container. The container will mainly test the PDE and TTS of the PMTs, as well as the dark count rate and the pre- and after-pulse rates.

1.2.2 Scanning station

The container approach is not sensitive to inhomogeneities of characteristics along the PMT's photocathode surface. Since all of the measurements in the container are performed in a constantly compensated magnetic field at the level of a few μT , it does not allow for the testing of a PMT's magnetic field sensitivity. In order to obtain these measurements a sampling of about a thousand PMTs will be tested more precisely. A special setup, called the scanning station, was designed and produced at the Joint Institute for Nuclear Research (see Fig. 1.3). The scanning station is placed in a light-tight dark room. In order to adjust/compensate for the EMF inside the black room Helmholtz coils are installed within the walls, floor and ceiling.

The core of the scanning station is a rotating frame with 7 stabilized compact pulsed light generators that are placed at different zenith angles. The frame is rotated by a step motor and covers all 360° azimuthal angles. A support system that holds the PMT allows for rotations in different spatial positions in order to put the PMT into different orientations with respect to the magnetic

field provided by the dark room. It allows for the testing of individual PMTs in all relevant aspects by scanning the photocathode, and allows for an in-depth understanding of the performance of a PMT, and may identify any potential problems. [2]

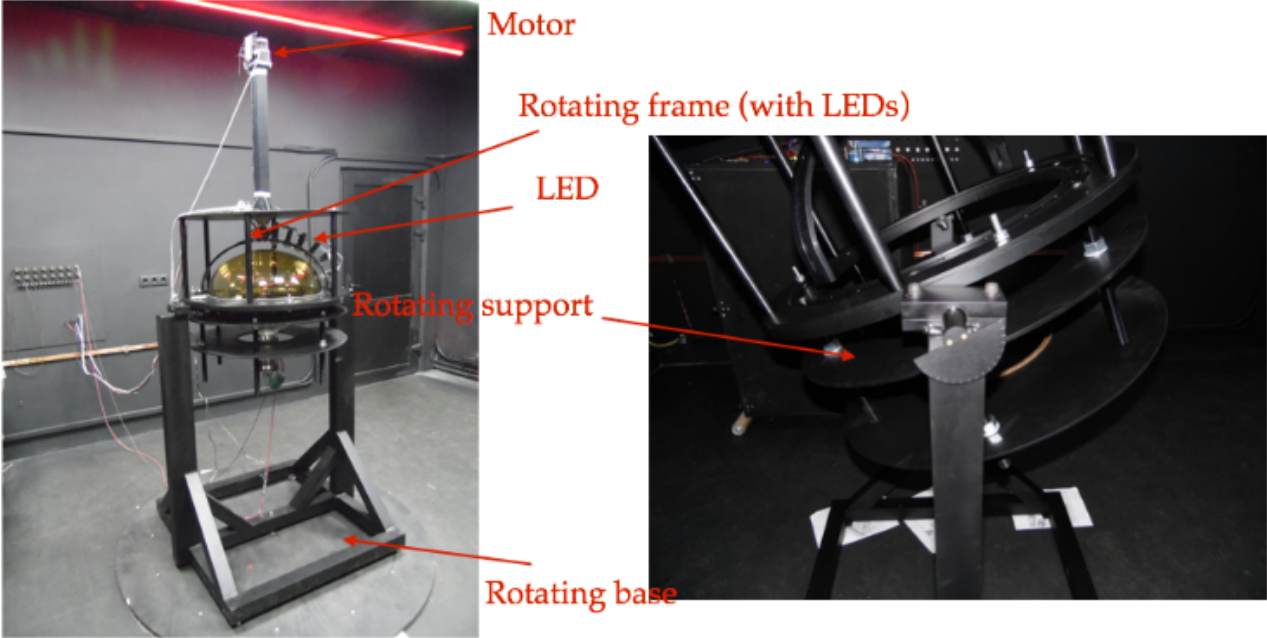


Figure 1.3: Scanning station general view in the dark room (left) and rotating support (right).

Chapter 2

Studying of the light field distribution in the container

The main requirement for a photomultiplier is Photo Detection Efficiency (PDE). If the PDE of a photomultiplier is less than 24% then it is not used. The average PDE for all 17000 PMTs should be at least 27%. Theoretically, the average PDE from all points of the photomultiplier is given by

$$\overline{PDE} = \iint PDE(\Omega, \alpha) \frac{d^2\Phi}{d\Omega d\alpha} d\Omega d\alpha = \iint A(\Omega, \alpha) P_{p.e.}(\Omega, \alpha) \frac{d^2\Phi}{d\Omega d\alpha} d\Omega d\alpha, \quad (2.1)$$

where $A(\Omega, \alpha)$ is photocathode absorption coefficient and $P_{p.e.}(\Omega, \alpha)$ is a probability to produce a photo-electron.

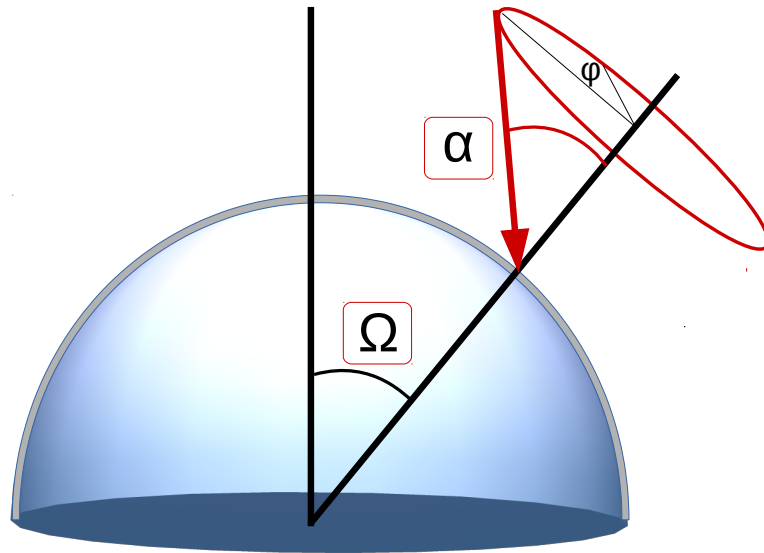


Figure 2.1: Definition of solid angles.

In (2.1) we don't know only the light field distribution $\frac{d^2\Phi}{d\Omega d\alpha}$ (LFD) in the container, that creates a teflon plate with a LED.

2.1 Preliminary measurements

First we need to know the characteristics of the devices we will work with.

2.1.1 Angular distribution of teflon plate

We placed the teflon plate far from the small PMT and using precise motions rotated a small photomultiplier around it. The calibrated LED illuminated the teflon plate from the other side close to it (See Fig. 2.2).

Theoretically the dependence of the intensity on the rotation angle for the point-like source should be expressed in terms of the squared cosine of this angle. But since the plate is not a point-like and isotropic light source this dependence is somewhat different (see Fig. 2.3).

Two maximums on the sides for measurements without the ASTD (near $\pm 50^\circ$) are visible because the photomultiplier starts to see not only the scattering plate but also the LED itself.

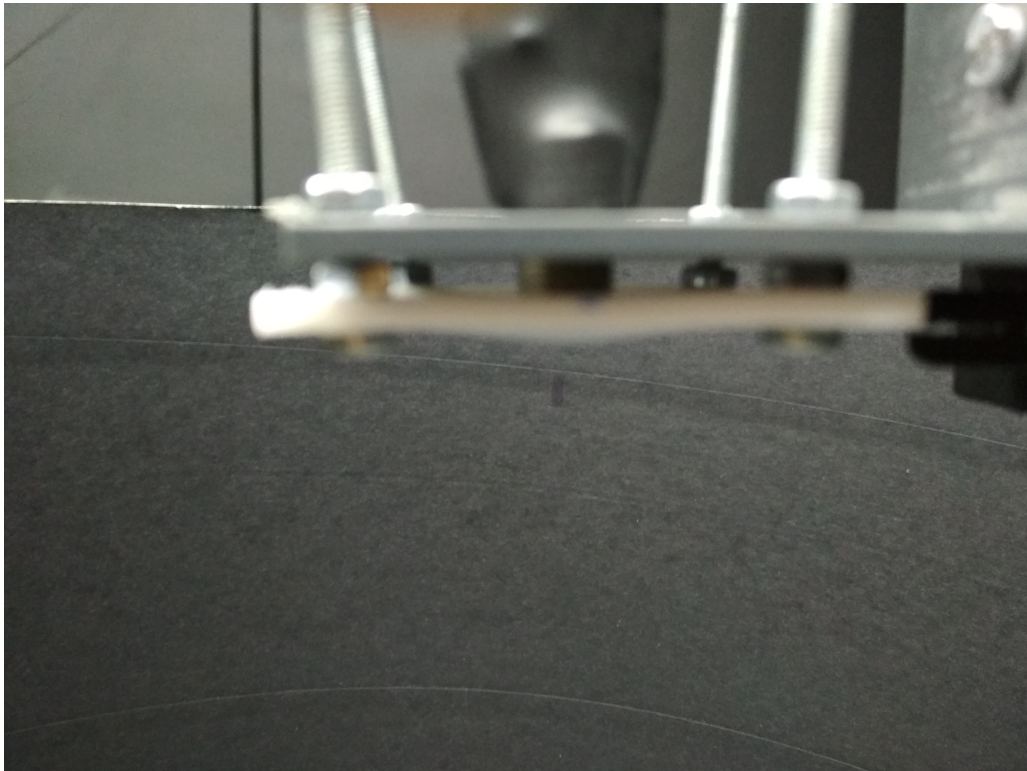


Figure 2.2: Teflon plate with LED.

2.1.2 The study of the angular transmittance of angular selective transmission device (ASTD)

Since a small photomultiplier (see Fig. 2.6) collects light in a large solid angle it is necessary to use an angular selective transmission device (ASTD) (Fig. 2.4), which will be put on a small PMT in order to obtain light only from the particular direction.

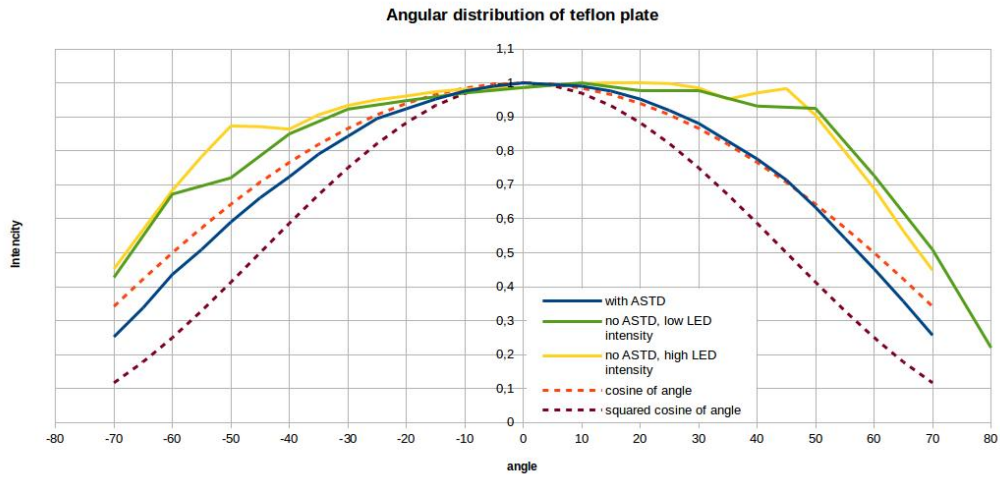


Figure 2.3: Angular distribution of teflon plate



Figure 2.4: Angular selective transmission device.

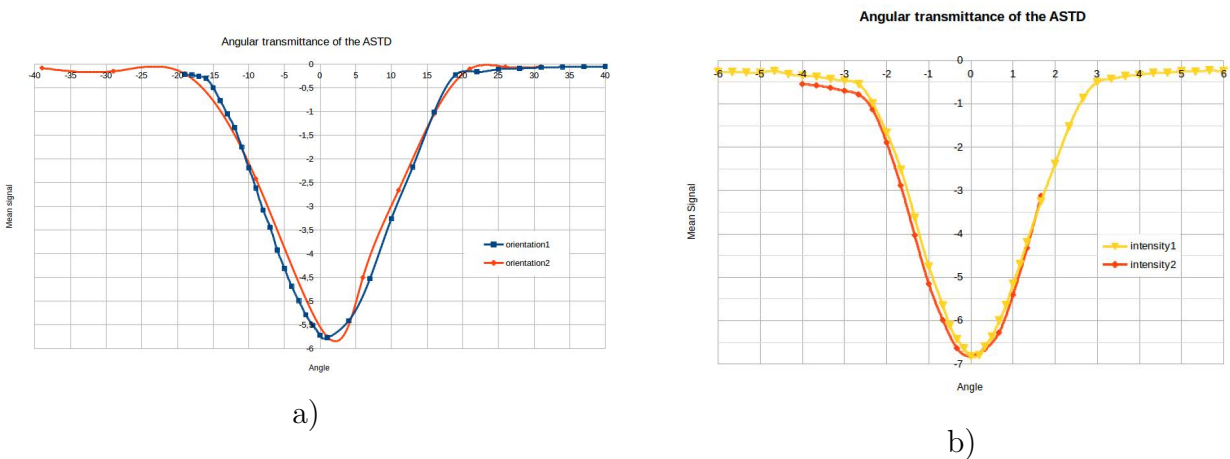


Figure 2.5: Angular transmittance of the ASTD.

To measure the angular transmittance of ASTD a small photomultiplier with it was rotated around the light source (calibrated LED) which was installed far from the small PMT in order to create a parallel beam of light.

We made the measurements for 2 different intensities of LED and for 2 different orientations of ASTD (the intensity in this case was the same for both measurements). The results are presented on Fig. 2.5a and Fig. 2.5b.

Concerning these graphs the angular transmittance of the ASTD is $\pm 1.5^\circ$. This result doesn't depend on the intensity of light (what is obvious) and slightly depends on the orientation of the ASTD because it is not ideal.

2.2 Small PMT approach

In this approach measurements were made by using a small photomultiplier (Fig. 2.6). With the help of a special arc (Fig. 2.7) the necessary angles corresponding to the zenith angle at the large photomultiplier were exposed.

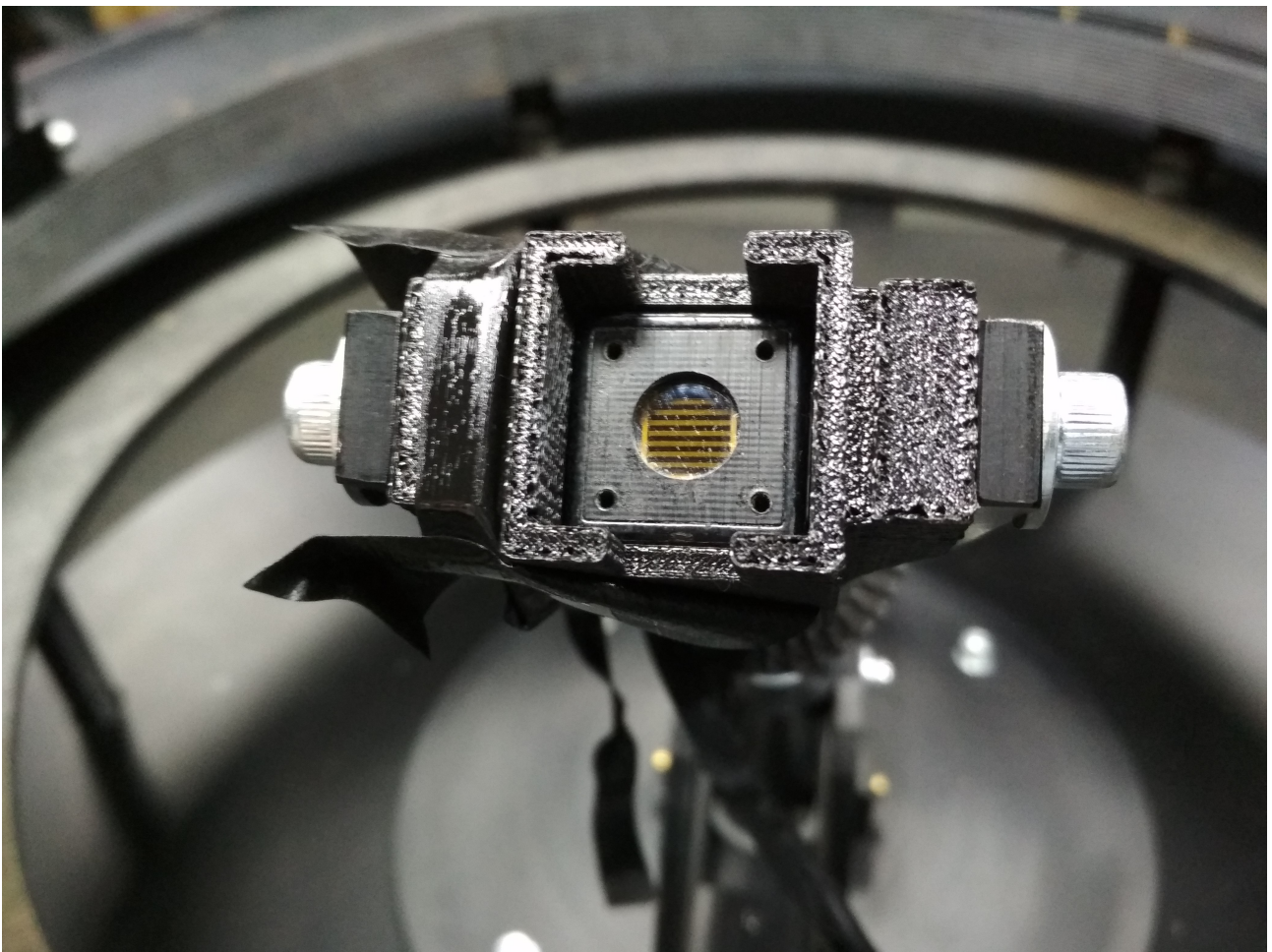


Figure 2.6: Small PMT.

Initially we wanted to make measurements for the zenith angles from 0° to 80° in increments of 5° . For each zenith angle it was necessary to make at least 156 measurements because each angle α corresponds to the cone of light with different polar angles φ (see Fig. 2.1). After we had started doing this it became clear that it would take a very long time, so it was suggested to make the same measurements with the camera. But still it was decided to carry out a complete



Figure 2.7: Special arc.

series of measurements for a zenith angle of 60° for further comparison of the results obtained by a photomultiplier and by a camera.

The results are presented on Fig. 2.8. The unusual shape of the curves from the angle φ from 120° to 240° for the α from 5° to 20° is due to the presence of a fold on white tyvek (that is, we get over the fold and there is lighter or under the fold, where it is darker). Some graphics (for example, for $\alpha = 25^\circ$) start with a steep dip, this is because the small photomultiplier looks at the black paper or the ceiling.

An interesting area is the $\alpha = 60^\circ$. The graph shows the values for ϕ from 30° to 330° because at $\varphi = 0^\circ$ the small PMT looks directly at the source. The number of photoelectrons that shows a small photomultiplier at this point is 72.71, which exceeds the characteristic value for other angles by 300–400 times. Given such a big difference the question arises, what is the overall contribution of the white tyvek relative to the light source.

From these measurements it can be concluded that if the main contribution to the light field is made by the source, rather than reflections from the white tyvek, then the container approach does not satisfy the requirements set to it (that is, it is not sensitive to the side surfaces of the large PMT, which are very important for the propagation of light in water, as in JUNO).

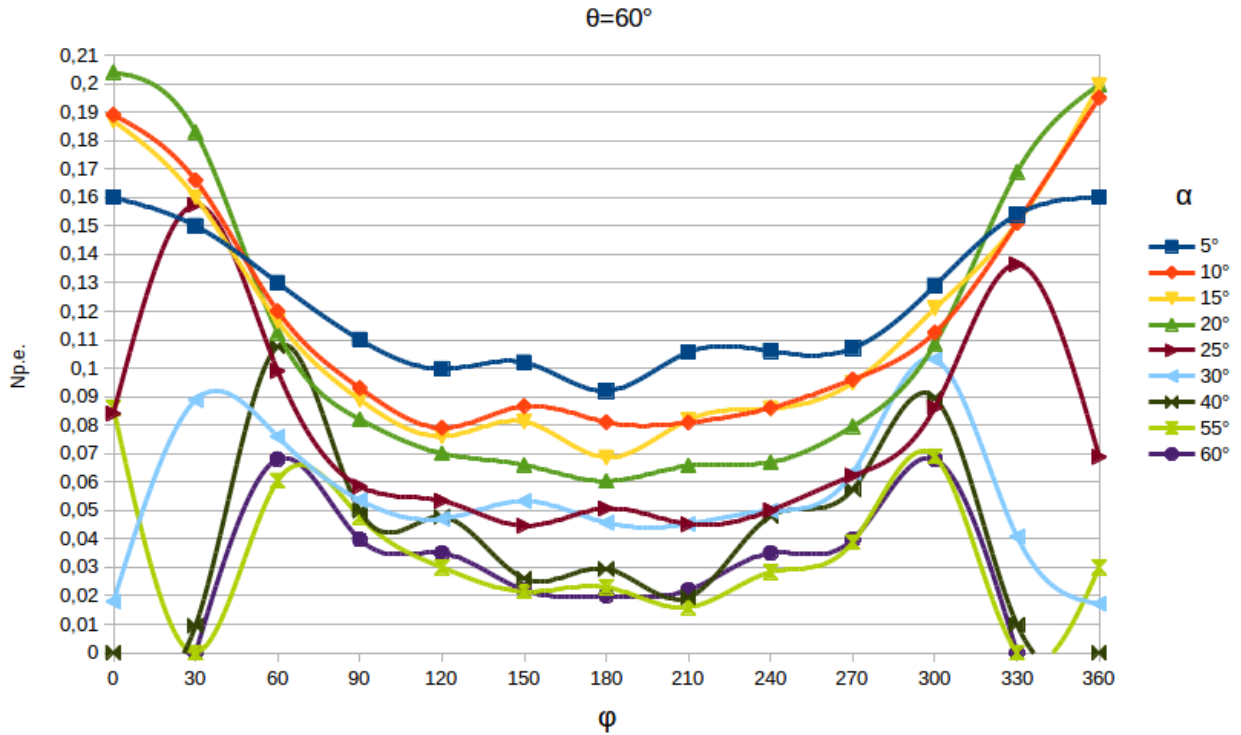


Figure 2.8: Measurements made by small PMT.

2.3 Camera approach

In this approach, a Sony Alpha NEX-F3 camera was used to measure the LFD. The images were taken at an exposure of 13 seconds and ISO 6400. These parameters were chosen so that the intensity of the blue light (our LED wavelength is 425 – 430 nm) did not exceed 225 conventional units. After 225 there is a highly nonlinear region (it is very close to the saturation zone) where it is impossible to work.

2.3.1 The construction of a characteristic curve between the values of a small PMT and the camera

To correlate the values obtained from the small PMT and from the camera a characteristic curve of the latter is needed. For such measurements a special setup (see Fig. 2.9) was assembled on the optical table (Standa).

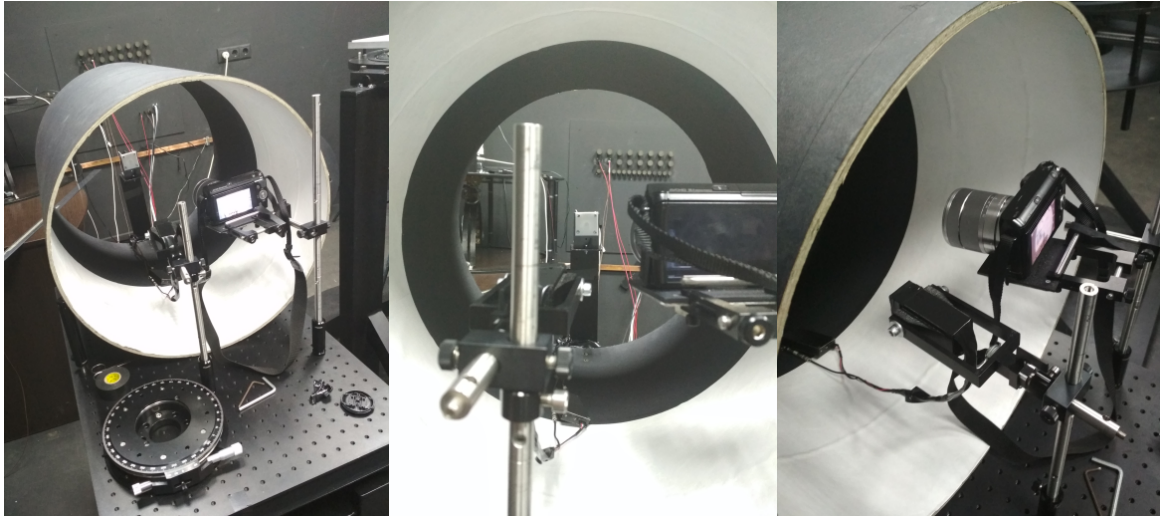


Figure 2.9: The construction for measuring the characteristic curve.

To construct the curve the camera and the small PMT were placed at the same distance from the light source (calibrated LED). With the help of special software the intensity of the source was changed. Exposure of the camera was 0.25 seconds in order to correlate the dynamic range of the camera with the small PMT.

The results are presented on Fig. 2.10. Since the camera is linear by the exposure and the small photomultiplier is linear by the light variation, we can use the curve for any parameters of the measured system.

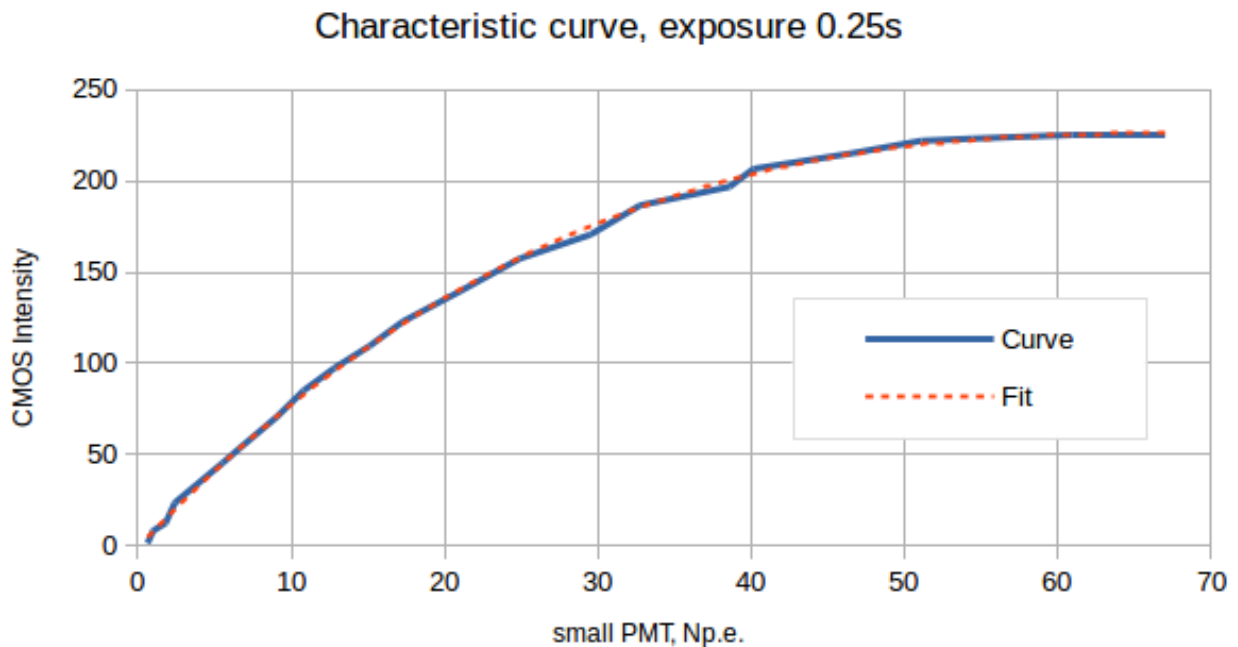


Figure 2.10: The characteristic curve of the camera.

2.3.2 Production and processing of photos

For measurements using a camera, there was a modified setup made at JINR, so that the camera could be fixed to the cylinder (Fig. 2.11). Also, the angle of the camera solution was measured which was $\pm 24^\circ$ vertically and $\pm 33^\circ$ horizontally.

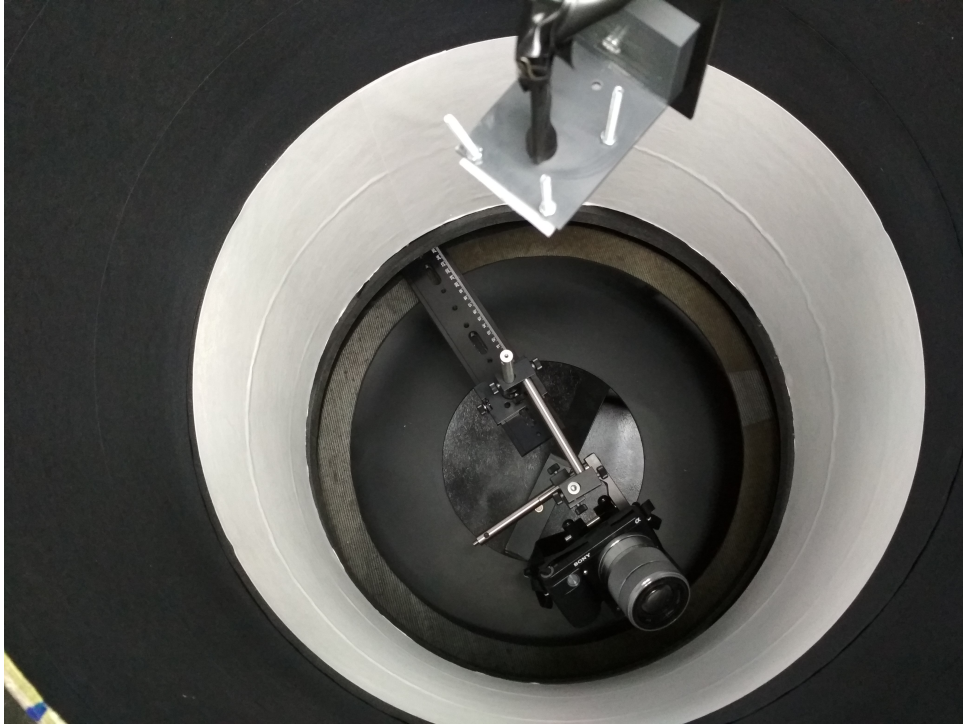


Figure 2.11: Camera setup.

Photographs of the light field were taken in increments of 10° along the zenith angle. For each zenith angle 3 photographs were taken. The first is normal to the surface, and two more are offset with respect to the angle of $\pm 20^\circ$ to capture the α angle from 0° to 40° inclusive (Fig. 2.12).



a) $\alpha = +20$ deg



b) $\alpha = 0$ deg



c) $\alpha = -20$ deg

Figure 2.12: Sample photos.

After the photos are received they must be connected (Fig. 2.13). Cross-stitching of photographs was done manually in the GIMP software. In the future it is planned to put the reference points on the tyvek for greater accuracy.

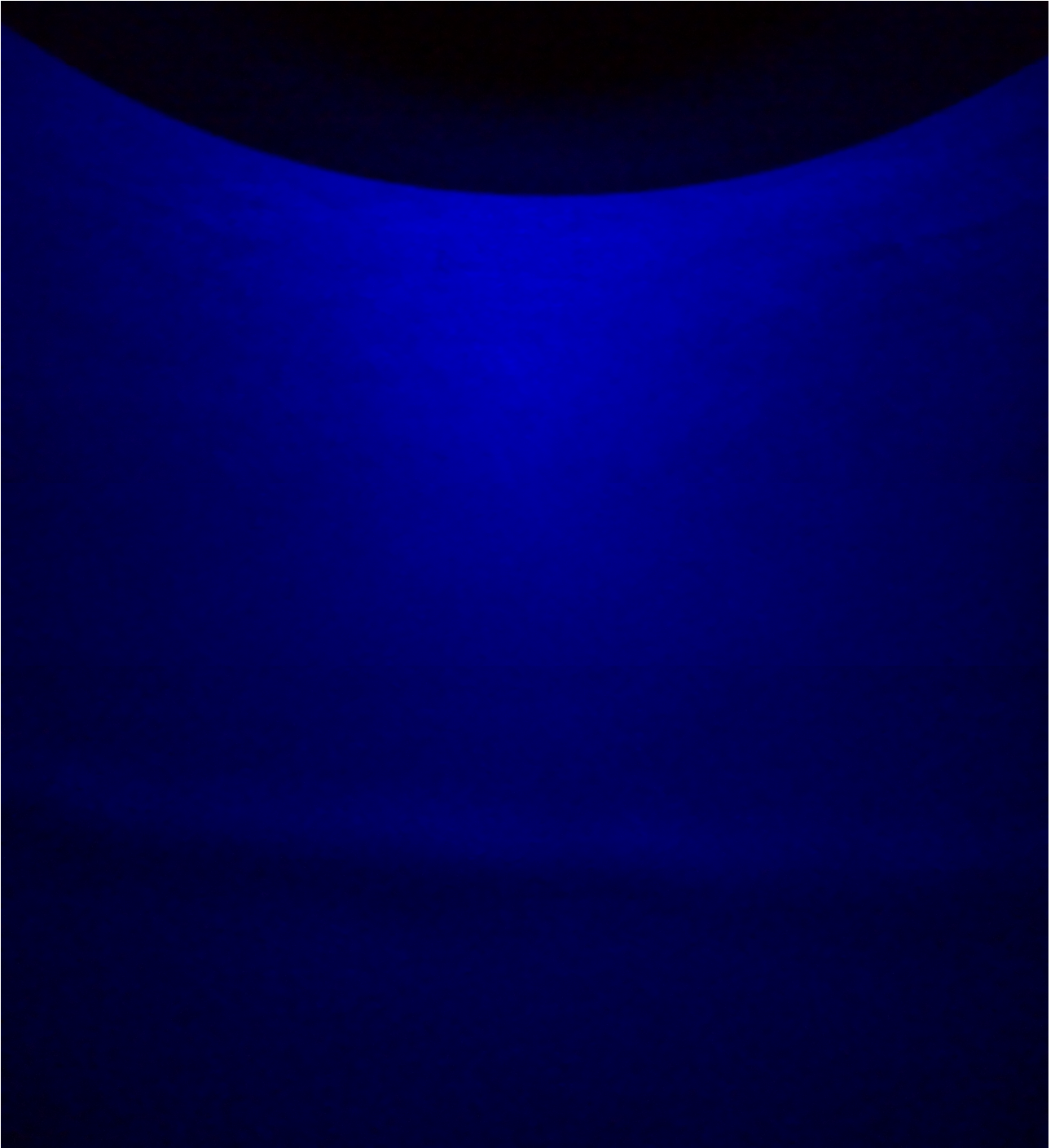


Figure 2.13: Example of a stitched photo.

For further processing of photographs a program was written on Python. The result of processing is the picture of the intensity in Cartesian (Fig. 2.14) and in polar (Fig. 2.15) coordinates. For the polar coordinates we averaged over the angle φ in increments of 1° and over $\cos \alpha$ in increments of 0.001. The photographs also show a fold on Tyvek that was discussed earlier for measurements with PMT.

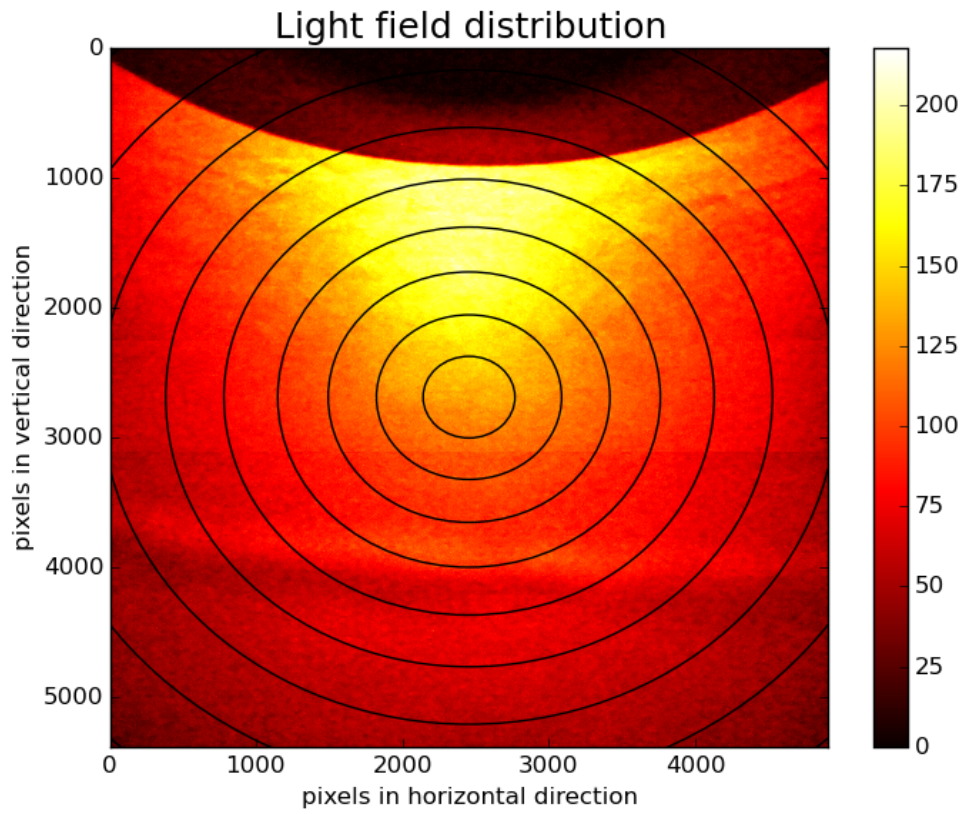


Figure 2.14: Cartesian coordinates. One circle corresponds to an alpha angle of 5 degrees.

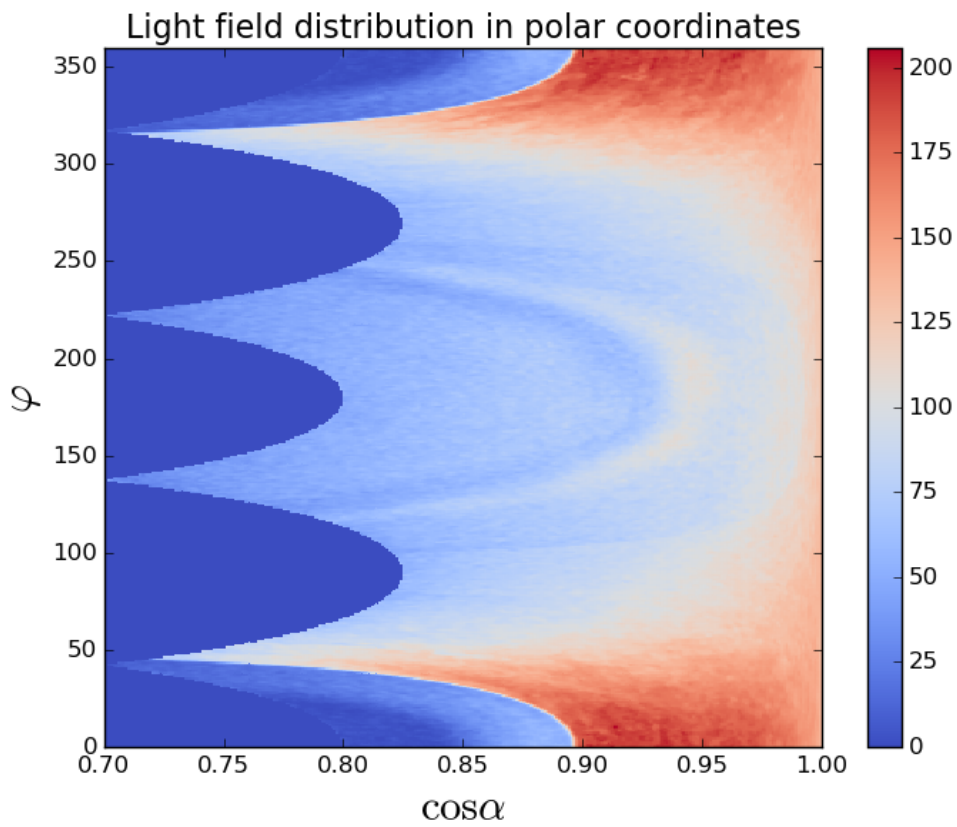


Figure 2.15: Polar coordinates.

The next step in the processing was the conversion of the camera intensities into photoelectrons for which the characteristic curve obtained earlier was used. The results are presented on Fig. 2.16.

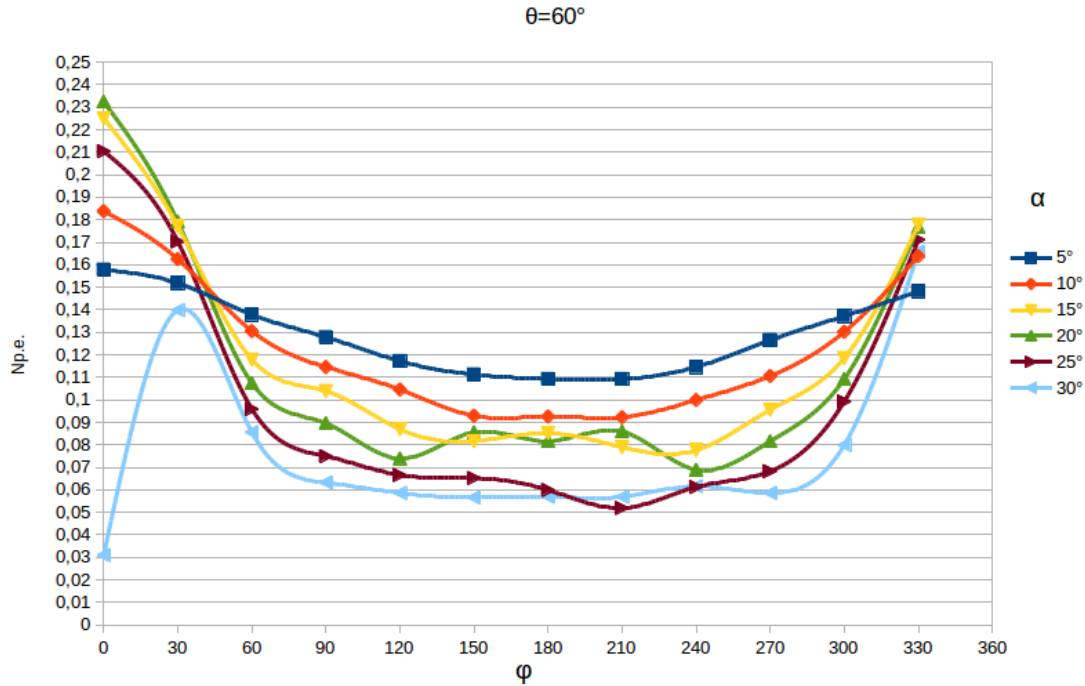


Figure 2.16: Measurements made by camera.

Comparing the data obtained with a small photomultiplier and a camera you can see that the general behavior of the curves is the same (compare Fig. 2.8 and Fig. 2.16), but we did not get the camera to the right zenith angle of the large PMT. To avoid this one needs to set the reference points on white tyvek with which you can accurately fall into the right angle and increase the accuracy of the stitching.

2.4 Estimation of the contribution to the LFD by diffuse light from tyvek

After we have obtained measurements for a zenith angle of $\theta = 60^\circ$ we can evaluate the effect of light scattered by tyvek on the distribution of the light field.

In the Table 2.1 the distribution of the light field supplemented to the alpha range from 70° to 90° is provided. The data points were extrapolated from the considerations that light from tyvek does not change much at these angles (we can use the same data for angles from 60° to 90°), and at the ϕ angle 0° , 30° and 300° degrees, a small photomultiplier looks at the ceiling and as a result does not see any light.

Table 2.1: The supplemented distribution of the light field

α/φ	0	30	60	90	120	150	180	210	240	270	300	330
0	0.13											
5	0.16	0.15	0.13	0.11	0.10	0.10	0.09	0.11	0.11	0.11	0.13	0.15
10	0.19	0.17	0.12	0.09	0.08	0.09	0.08	0.08	0.09	0.10	0.11	0.15
15	0.19	0.16	0.12	0.09	0.08	0.08	0.07	0.08	0.09	0.95	0.12	0.15
20	0.20	0.18	0.11	0.08	0.07	0.07	0.06	0.07	0.07	0.08	0.11	0.17
25	0.08	0.15	0.10	0.06	0.05	0.04	0.05	0.05	0.05	0.06	0.09	0.14
30	0.02	0.09	0.08	0.05	0.05	0.05	0.05	0.05	0.05	0.06	0.10	0.04
40	0	0.01	0.11	0.05	0.05	0.03	0.03	0.02	0.05	0.06	0.09	0.01
55	0.06	0	0.06	0.05	0.03	0.02	0.03	0.02	0.03	0.04	0.07	0
60	72.71	0	0.07	0.04	0.04	0.02	0.02	0.02	0.04	0.04	0.07	0
70	0	0	0.07	0.04	0.04	0.02	0.02	0.02	0.04	0.04	0.07	0
80	0	0	0.07	0.04	0.04	0.02	0.02	0.02	0.04	0.04	0.07	0
90	0	0	0.07	0.04	0.04	0.02	0.02	0.02	0.04	0.04	0.07	0

Further, for the estimation we used the following approximations:

1. Light field $f(\alpha, \varphi)$

- is the same within the intervals for the α angle,
- is the same within the intervals for the φ angle,
- is normalized to 1 for a zenith angle $\theta = 60^\circ$.

2. Coefficient of absorption of photocathode $A(\alpha)$

- is the same within the intervals for the α angle.

3. Photo Detection Efficiency

- is defined for the angle θ and does not depend on the angles of incidence α and φ .

A signal that will produce a large PMT with such light parameters (Table 2.1) is determined by the formula:

$$S = \int_0^{2\pi} d\varphi \int_0^{\pi/2} \sin \alpha A(\alpha) f(\alpha, \varphi) PDE(\theta) d\alpha. \quad (2.2)$$

The integrated over the angle φ signal will be distributed along the α rings (we call the rings the following region $[\alpha - \delta\alpha; \alpha + \delta\alpha]$) in a percentage ratio as follows:

Table 2.2: The percentage contribution of each ring to the distribution of the light field

α	0	5	10	15	20	25	30	40	55	60	70	80	90
S	0.02	0.13	0.24	0.57	0.44	0.39	0.55	0.84	0.63	95.13	0.59	0.48	0

Thus, the distribution of the light field in the container is highly heterogeneous, and the percentage of light reflected from tyvek is less than 5 percent, which does not meet the requirements.

Conclusion

During the summer student's practice, the following was done:

1. The characteristics of the container were measured — the angular distribution of the teflon plate in the cylinder.
2. To measure the light field inside the container, two methods were proposed:
 - Using a small PMT with a ASTD, for which its transmittance was also measured;
 - With the camera: this approach still needs to be improved.
3. An estimate of the influence of tyvek on the distribution of the light field in the cylinder of the container was given.

Bibliography

- [1] An F. Neutrino Physics with JUNO / F. An, G. An, Q. An, et al. // arXiv:1507.05613v2 [physics.ins-det]
- [2] Anfimov N. Large photocathode 20-inch PMT testing methods for the JUNO experiment / N. Anfimov // arXiv:1705.05012 [physics.ins-det]